Effects of changes in CO2, climate, and land use on the carbon balance of the land biosphere during the 21st century

Christoph Müller, Bas Eickhout, Sönke Zaehle, Alberte Bondeau, Wolfgang Cramer, Wolfgang Lucht

Effects of changes in CO_2, climate, and land use on the carbon balance of the land biosphere during the 21st century

Christoph Müller*†, Bas Eickhout‡, Sönke Zaehle*§, Alberte Bondeau*, Wolfgang Cramer*, and Wolfgang Lucht*

* Potsdam Institute for Climate Impact Research, PO Box 60 12 03, 14412 Potsdam, Germany

† International Max Planck Research School on Earth System Modeling, Bundesstr. 53, 20146 Hamburg, Germany

‡ Netherlands Environmental Assessment Agency (RIVM/MNP), Global Sustainability and Climate, P.O.Box 303, 3720 AH BILTHOVEN, The Netherlands

§ current address: LSCE, Orme des Merisiers, Bat. 712, 91191 Gif-sur-Yvette, France

Keywords: climate change, land-use change, carbon cycling, 21st century, SRES

Correspondence: Christoph Müller,

Potsdam Institute for Climate Impact Research,

PO Box 60 12 03,

14412 Potsdam,

Germany,

fax: +49 331 2882640,

e-mail: Christoph.Mueller@pik-potsdam.de

Running Title: Effects of CO_2, climate, and land use

Abstract

We studied the effects of climate and land-use change on the global terrestrial carbon cycle for the 21st century. Using the process-based land biosphere model (LPJmL), we mechanistically simulated carbon dynamics for natural and managed lands (agriculture and forestry) and for land-use change processes. We ran LPJmL with twelve different dynamic land-use patterns and corresponding climate and atmospheric CO_2 projections. These input data were supplied from the IMAGE 2.2 implementations of the IPCC-SRES storylines for the A2, B1, and B2 scenarios. Each of these SRES scenarios was implemented under four different assumptions on spatial climate patterns in IMAGE 2.2, resulting in twelve different Earth System projections. Our selection of SRES scenarios comprises deforestation and afforestation scenarios, bounding a broad range of possible land-use change. Projected land-use change under different socio-economic scenarios has profound effects on the terrestrial carbon balance: While climate change and CO_2 fertilization cause an additional terrestrial carbon uptake of 105-225 PgC, land-use change causes terrestrial carbon losses of up to 445 PgC by 2100, dominating the terrestrial carbon balance under the A2 and B2 scenarios. Our results imply that the potential positive feedback of the terrestrial biosphere on anthropogenic climate change will be strongly affected by land-use change. Spatiotemporally explicit projections of land-use change and the effects of land management on terrestrial carbon dynamics need additional attention in future research.

1 Introduction

Climate change during the 21st century will be determined by the trajectory of greenhouse gas (GHG) concentrations, biophysical interactions with the earth's surface and feedbacks with the Earth System. Changes in atmospheric CO_2 concentration are the net result of emissions from fossil fuel combustion, cement production, and carbon exchange with oceans and land ecosystems. Land-use and land-cover change affects the carbon balance of the terrestrial biosphere [e.g., Smith et al., 1993; Houghton, 1999; Foley et al., 2005] and influences the distribution of terrestrial carbon sources and sinks [Canadell, 2002; Dargaville et al., 2002]. The terrestrial carbon balance therefore is a function of socio-economic dynamics [Lambin et al., 2001] as well as biogeochemical processes in plants and soil [McGuire et al., 2001]. Recent studies on the future development of the global carbon cycle focus on effects of climate change projections [Schaphoff et al., 2006] and on the feedback between climate and the carbon cycle [Cox et al., 2000; Dufresne et al., 2002; Friedlingstein et al., 2003; Berthelot et al., 2005; Matthews et al., 2005]. In these studies, carbon emissions from land-use change are included in the driving carbon emission scenarios.

At local and regional scales, however, past and future land use is found to significantly affect the carbon cycle by changing carbon cycle processes [Haberl et al., 2001; Achard et al., 2002; Ometto et al., 2005; Schröter et al., 2005; Smith et al., 2005; Smith et al., 2006; Zaehle et al., 2007]: Soil- and vegetation carbon pools change after deforestation [Fearnside, 2000] and afforestation [Caspersen et al., 2000; Guo and Gifford, 2002], and carbon sequestration under cultivation is reduced as assimilated carbon is removed at harvest [Post and Kwon, 2000], accelerating carbon turnover times [Gitz and Ciais, 2003]. Finally, differences in phenology and crop management [Lal, 2004] have been found to have spatially varying effects on net primary production (NPP) and carbon fluxes [DeFries, 2002; Jones and Donnelly, 2004; Bradford et al., 2005].

In spite of this knowledge, future changes in land-use are rarely addressed explicitly in carbon cycle studies at the global scale. Reasons for this are the large uncertainties connected with the drivers of land-use change such as population growth or requirements for cultivated land [Levy et al., 2004b] and the absence of numerical modules for carbon dynamics under cultivation in most global process-based models. Early approaches to study the effects of future land-use change on the carbon cycle at the global scale focused mainly on selected aspects of land-use change. For example, House et al. [2002] approached the topic by studying total deforestation and total afforestation in a bookkeeping model and DeFries [2002] analyzed the effects of past and future land-use changes on NPP. In the pan-tropical region, Cramer et al. [2004] studied deforestation by extrapolating trends of twentieth century deforestation rates. They employed different climate scenarios to account for uncertainties in climate change projections. Levy et al. [2004a] derived trends of land-use change from SRES storylines [Nakicenovic and Swart, 2000] that included feedbacks within the society-biosphere-atmosphere system. Sitch et al. [2005] employ spatially explicit land-use patterns also derived from the SRES storylines to drive their coupled climate-biosphere model (CLIMBER2-LPJ).

The results reported in these studies are ambiguous and do not allow for a comprehensive analysis of the role of land-use change for the terrestrial carbon cycle. Besides the underlying uncertainties in future projections of land-use patterns [Levy et al., 2004b] and climate change [Murphy et al., 2004], there is disagreement in the response of the terrestrial biosphere to land use and land-use change as simulated in different global model applications. For example, Levy et al. [2004a] and Sitch et al. [2005] attribute only small carbon fluxes to land-cover and land-use changes that only marginally affect the terrestrial carbon balance. Levy et al. [2004a] report that land-use emissions are considerably smaller than the effects of CO_2 fertilization and climate change. They find land-use change to be a constant carbon source of approximately 1 PgC/a only under the B2 scenario. Under the A1, A2, and B1

scenarios, land-use change processes do not affect the terrestrial carbon balance in their study, although the cultivated area is reduced by ~50% under their A1 and A2 scenarios. Sitch et al. [2005] also find that the terrestrial biosphere is a net carbon sink under all SRES scenarios they studied (A1b, A2, B1, and B2). Gitz and Ciais [2004] and Cramer et al. [2004], on the other hand, find land-cover changes to significantly affect the terrestrial carbon budget of the 21st century. Gitz and Ciais [2004] report land-use changes from 1990 to 2100 under the A2 SRES scenario to be responsible for carbon emissions of at least 305 PgC. Cramer et al. [2004] find that tropical deforestation alone may transfer 100 to 370 Pg of terrestrial carbon to the atmosphere over the 21st century.

In this study, we make use of 12 future Earth System projections, to analyze the effects of atmospheric CO_2 concentrations, climate and land-use change as simulated by the IMAGE 2.2 model (Integrated Model to Assess the Global Environment) for the SRES scenario storylines A2, B1, and B2 [IMAGE team, 2001]. This selection of SRES scenarios comprises scenarios of substantial deforestation (A2), of afforestation (B1), and of moderate changes (B2). We employ the process-based land biosphere model LPJmL ("LPJ for managed Land") [Bondeau et al., 2007] to explicitly simulate carbon dynamics of natural and managed land (agriculture, forestry) and under land-use changes processes. The terrestrial carbon cycle is represented in IMAGE 2.2 in simplified form only [IMAGE team, 2001], as its dynamics are not in the main focus of the IMAGE model. Thus, we are studying the biospheric reaction to potential changes in climate, atmospheric CO_2 concentrations, and land-use in more detail here, going beyond the IMAGE-based study of Leemans et al. [2002]. Compared with other earlier approaches to account for land-use effects on the global terrestrial carbon cycle, we move one step forward by explicitly modeling the carbon dynamics of agricultural land and land-use change processes, using the LPJmL model. To our knowledge, this is the first study to address different climate and land-use change projections consistently in a DGVM to study

the effects on the global carbon cycle, explicitly accounting for carbon dynamics under cultivation.

2 Materials and Methods

2.1 Lund-Potsdam-Jena DGVM

The LPJmL model [Bondeau et al., 2007] is based on the LPJ-DGVM [Sitch et al., 2003], a biogeochemical process model that simulates global terrestrial vegetation and soil dynamics and the associated carbon and water cycles. For this, the processes of photosynthesis, evapotranspiration, autotrophic and heterotrophic respiration, including the effects of soil moisture and drought stress, as well as functional and allometric rules are implemented [Sitch et al., 2003; Gerten et al., 2004]. Net primary production (NPP, defined as gross primary production less autotrophic respiration) is allocated to the different plant compartments (vegetation carbon) and enters the soil carbon pools (including litter pools) due to litter-fall and mortality. Fire disturbance is driven by a threshold litter load and soil moisture function [Thonicke et al., 2001]. Runoff is generated if precipitation exceeds the water holding capacity of the two defined soil layers that supply water for evaporation from bare soil and for transpiration (interception loss from vegetation canopies is computed based on precipitation, potential evapotranspiration, and leaf area [Gerten et al., 2004]).

Natural vegetation is represented by 10 different plant functional types (PFTs), of which 2 are herbaceous and 8 woody. These may coexist within each grid cell, but their abundance is constrained by climatic conditions, by competition between the different PFTs for resources and space, and by the fractional coverage with agricultural vegetation. Vegetation structure responds dynamically to changes in climate, including invasion of new habitats and dieback.

The model has been extensively tested against field sites [Sitch et al., 2003; Cramer et al., 2004; Gerten et al., 2005; Zaehle et al., 2005], inventory data [Beer et al., 2006], satellite

remote sensing [Lucht et al., 2002; Wagner et al., 2003], atmospheric [Scholze et al., 2003; Sitch et al., 2003], and hydrological data [Gerten et al., 2004; Gerten et al., 2005].

In LPJmL, agricultural land use is simulated within the same framework using crop functional types (CFTs) [Bondeau et al., 2007]. The world's most important field crops as well as pastures are represented by a total of 13 different CFTs (temperate cereals, tropical cereals, rice, maize, pulses, temperate roots and tubers, tropical roots and tubers, soybean, sunflower, peanuts, rapeseed, managed C_3-grass, managed C_4-grass, see also Table 1) that can be simulated either with realistic water stress (rain-fed agriculture) or without (irrigated). Grid cells may fractionally consist of both natural and agricultural vegetation. Several agricultural crops may be present within the same grid cell with individual cover fractions that are prescribed by the land-use input data, while individual cover fractions of PFTs in natural stands are internally determined by LPJmL. Each CFT has its own specific stand and water budget so that they do not compete with each other or with natural vegetation.

LPJmL's crop modules simulate crop phenology, growth, and carbon allocation at a daily time step. Carbon is allocated to several plant compartments, including a storage organ that represents the economic yield at harvest. Carbon allocation to the different plant compartments is CFT specific and is affected by the plant's actual phenological state and water stress. The model estimates several crop variety-specific parameters as a function of climate, thereby taking into account the farmer's choice of a variety that is adapted to specific climatic environments in which they are cultivated. The implementation of the crop-specific processes is described in detail and compared

- against the USDA crop calendar [USDA, 1994] for sowing dates,
- satellite data [Myneni et al., 1997] for phenology,
- against FAO data [FAOSTAT data, 2005] for yields,

- against eddy flux measurements from three agricultural sites (Ponca and Bondville from the Ameriflux network (http://public.ornl.gov/ameriflux) and Jokioinen in Finland [Lohila et al., 2004]) for carbon fluxes

by Bondeau et al. [2007].

LPJmL allows for specifying several management options: Irrigation of crops is determined by the IMAGE land-use data, but is currently not constrained by water availability. As a consequence, irrigation is simulated as perfect on-demand irrigation. For the lack of appropriate input data, we here generally do not simulate intercrops and we remove crop residues after harvest. For a detailed description of the crop modules in LPJmL, see Bondeau et al. [2007].

Managed forests are simulated assuming competition between tree individuals as described in Sitch et al. [2003], but with a prescribed PFT composition. This PFT composition is derived from the PFT composition simulated by LPJ for the period of 1990-1999, considering the two tree PFTs with the largest fractional grid cell coverage in each individual grid cell. Harvesting of trees, and thus carbon removal, is modeled based on a prescribed rotation time of 100 years, and forest productivity [Zaehle et al., 2007]. 40% of the harvested carbon is respired directly (fuel wood, biomass burning etc.), 33% enters litter pools and 27% enter the product pools, based on the partitioning used by McGuire et al. [2001].

2.2 Data

LPJmL was driven by climate data from the University of East Anglia's Climatic Research Unit (CRU) climate data set [Mitchell et al., 2004], a monthly climatology of observed meteorological parameters, and annual atmospheric CO_2 concentrations [Keeling and Whorf, 2003] for the period from 1901-1999. For the period 2000 to 2100, we used data of twelve different scenarios supplied from the IMAGE 2.2 model [IMAGE team, 2001]. The IMAGE 2.2 model is a comprehensive Integrated Assessment Model that includes several sub-modules

to cover society, climate, and the biosphere as well as major feedbacks between these systems. The model has a geographical resolution of 0.5° × 0.5° longitude/latitude and supplies *inter alia* spatially explicit land-use, temperature, and precipitation patterns, global atmospheric CO_2 concentrations, and other parameters that are not used in this study. A detailed description of the IMAGE 2.2 model can be found in the publications of Alcamo et al. [1998] and IMAGE team [2001]. For this analysis, we used the A2 (economy oriented, regionally segregated), B1 (environment oriented, globalized), and B2 (environment orientated, regionally segregated) SRES scenarios [Nakicenovic and Swart, 2000; IMAGE team, 2001] to cover the range of different land-use and climate patterns (Table 2; Figure 1). The climate module of IMAGE simulates global climate change as changes in global mean temperature. This global-mean temperature change is used to generate spatially explicit temperature and precipitation patterns (0.5 × 0.5°) to drive other modules of IMAGE 2.2. For this, IMAGE employs the standardized IPCC scaling method [Carter et al., 1994], supplemented by the scaling method of Schlesinger et al. [2000] to take into account the non-linear climate effects of sulfate aerosols. In order to account for uncertainties in local climate change, four different GCM patterns were used to downscale the global-mean temperature change [IMAGE team, 2001]: HADCM2 [Mitchell et al., 1995], ECHAM-4 [Bacher et al., 1998], CGCM-1 [Boer et al., 2000], and CSIRO-MK12 [Hirst et al., 1996]. Owing to the feedbacks between climate, society, and biosphere that are implemented in IMAGE 2.2, these differences in climate patterns modify the temporal simulation of atmospheric CO_2 concentrations as well as climate and land-use patterns. As a consequence, each SRES scenario is implemented four times, with differences in climate, land use, and atmospheric CO_2 concentrations. The land-use patterns for each SRES scenario are globally (Figure 1) and regionally similar but differ locally (Figure 2). The monthly IMAGE climatology was supplied for the years 2000, 2025, 2050, 2075, and 2100. To generate time series for the period 2000-2100 with annual values for each month, we interpolated linearly between the 25-year intervals. To account for interannual

climate variability, we repeatedly added the detrended 30-year variability of the 1970-1999 CRU data (absolute variability for temperature, relative variability for precipitation) to the linearly interpolated time series. For sunshine data, we used the CRU data for 1970-1999 repeatedly for the simulation period 2000-2100. We kept the number of monthly rain days constant after 1999 at the 1970-1999 average of each month.

IMAGE data on land-use and atmospheric carbon dioxide concentrations were supplied in 5-year intervals, which we interpolated linearly to generate annual time series. IMAGE land-use data are supplied only after 1970. However, other global historic land-use data sets available do not match the IMAGE land-use pattern in 1970. To account for land-use changes between 1901 and 1969, we derived regional trends for cropland and pasture areas from the HYDE database [Klein Goldewijk, 2001], which is also based on FAO statistics but differs in spatial pattern from the IMAGE land-use data for 1970. Scaling the IMAGE land-use pattern of 1970 with these trends, we generated annual land-use input data for the period 1901-1969, which are equal for all 12 scenarios. Each model run was initialized by a spin-up of 900 years duration during which the first 30 years of the climate data set were repeated cyclically. During the spin-up, the land-use pattern was kept static at the values of 1901 to bring all carbon pools into equilibrium.

IMAGE 2.2 supplies land-use data for 5 categories (timber, extensive grassland, regrowth, cropland, and natural vegetation), which we mapped to LPJmL land-use categories and CFTs (see Table 1). The different land-cover types supplied by IMAGE for natural vegetation were ignored, as the composition of natural vegetation is internally determined by LPJmL. Total cropland consists of a grid cell specific mixture of crop types. Data on crop type mixtures for each grid cell were supplied for 1970 and 2100 only. To account for changes in crop mixtures over time, we interpolated linearly between 1970 and 2100. We kept crop shares constant in grid cells that are not agriculturally used in either 1970 or 2100 and

assigned regional default crop mixes to grid cells that are not agriculturally used in 1970 and 2100 but in between.

We assigned the 19 IMAGE crop type categories to the different CFTs implemented in LPJmL as specified in Table 1 and restricted the crop mix to the 3 most dominant CFTs. For aggregate crop categories that can be represented by several CFTs in LPJmL (e.g., IMAGE *oil crops* can be represented by the CFTs *sunflower*, *soybean*, *rapeseed*, and *peanut*) the most productive CFT was selected based on the average productivity as simulated by LPJmL for the period of 1990-1999. *Woody biofuels* are considered crops in IMAGE but are simulated as *managed forests* in LPJmL (see Table 1).

2.3 Experimental setup and simulations

We performed simulations with LPJmL for all 12 scenarios (3 SRES scenarios A2, B1, and B2, each in four implementations with different GCM climate patterns) on a regular global grid with 0.5° × 0.5° spatial resolution. The main characteristics of each scenario are summarized in Table 2 (see also Figure 1). We analyzed the marginal effects of climate and land-use changes on the terrestrial carbon balance in two separate simulations: In the first, we used static land-use patterns after 1970, changing only climate and atmospheric CO_2 concentrations during the scenario period (1970-2100), hereafter referred to as CC. In the second, we also changed land-use patterns after 1970, according to the scenario settings, hereafter referred to as CCL. Consequently, the difference between the CC-simulation and the CCL-simulation of each scenario (SRES + GCM) is completely attributable to the effects of land-use change during 1970-2100.

3 Results

3.1 Effects of changes in climate and atmospheric CO_2 concentrations

Increasing atmospheric CO_2 concentrations and associated climate change caused increased biospheric carbon sequestration, summing up to 105 to 225 PgC additionally stored in the biosphere by 2100 (Figure 3b). The additional amount of carbon in 2100 relative to 1970 stored in vegetation is double than that in the soil.

NPP, heterotrophic respiration (R_h), and the harvested carbon flux (HC, defined as sum of decaying wood products from the product pools and harvesting flux from grasslands and croplands, including the removed residuals in PgC/a) increased under all scenarios (Figure 4b; see Table 3 for an overview). The steady increase in NPP is followed by an increase in R_h as the litter input increases with NPP. Under the four A2 scenarios, the effects of CO_2 fertilization and climate on NPP are greater compared to the increases in R_h as shown in Figure 4b. HC resulted in increases for all scenarios, even though land-use patterns were not changed (Table 3, Figure 4b). This increase in HC is due to the enhancement of crop productivity at the global scale, which is caused by climate change and CO_2 fertilization. Wildfire carbon emissions increase from 3.8 PgC/a in the 1970s, which is close to the figures reported by Andreae and Merlet [2001] for the late 1990s, to 5.2 (+/- 0.2) PgC/a by 2100 (Table 3).

Balancing these carbon fluxes, the net ecosystem exchange flux (NEE, defined as R_h + fire emissions + HC – NPP) increases under the A2 scenarios to up to –2.5 PgC/a (carbon sink, negative fluxes denote a net C flux from the atmosphere to the terrestrial biosphere). Under the B1 and B2 scenarios, NEE remains about constant around -1.0 PgC/a. The superimposed interannual 30-year CRU-climate variability (see section 2.2) and the

differences between the different CGM patterns can be clearly recognized in the temporal dynamics of NEE (Figure 5b).

Under all scenarios, carbon is sequestered in the biosphere in all regions as shown in Figure 6d,e,f. However, NEE increases (i.e. less sequestration or more emissions) in central Africa under the B1 and B2 scenarios as well as some parts of Siberia under the A2 and B2 scenarios (Figure 6 d,e,f). Regional differences between the different GCM-patterns used are minor but there are some local differences, especially between the different A2 scenarios (e.g., in Siberia and northern America).

3.2 Effects of land-use change

We derive the marginal effect of land-use change as the difference between the CCL and the CC scenarios. All scenarios start with agricultural expansion and deforestation in the late 20th and early 21st century, causing carbon emissions to the atmosphere (Figure 5c). The shape of the emission curve corresponds to the rate of deforestation. For the A2 scenarios, deforestation rates (including clear-cuts for the expansion of managed forests) increase until mid 2010s to up to 0.34 million km²/a, decline to 0.11 million km²/a in 2040 and increase again to up to 0.28 million km²/a by 2100 (see also Figure 1). NEE closely follows these changes in deforestation rates under all scenarios (Figure 5c), but with a temporal lag of a few years, since the soil carbon pools react slowly to the changes in vegetation cover. The same correlation can be observed for the B1 scenarios (under which deforestation rates of the 21st century are always lower than during the late 20th century and switch to afforestation by 2015) and the B2 scenarios (under which deforestation rates also peak in the 2010s, decline to zero by 2030 and switch to afforestation by 2080). Under the B1 and B2 scenarios, the temporal lag between changes in deforestation rates and the NEE response can be seen most clearly in Figure 5c when the scenarios change from deforestation to afforestation: Although afforestation starts in the 2010s (B1) and 2030s (B2, see Figure 1) and the trend of NEE turns

around shortly thereafter, land-use change causes a carbon sink not until the 2050s and 2080s respectively (Figure 5c).

Accordingly, total terrestrial carbon stocks decline under all scenarios due to land-use change (Figure 3c). Under the A2 scenarios, up to 445 PgC is lost by 2100. Under the B1 scenarios, terrestrial carbon stocks decrease by 120 PgC from 1970 to 2100, although carbon stocks increase after 2050 (reflecting afforestation). For the B2 scenarios, total terrestrial carbon is reduced by 205 PgC by 2080 and remain about constant thereafter.

NPP decreases slightly in the 21st century due to land-use change (Figure 4c), which does not include changes in management, such as new varieties or changes in fertilization. The response of R_h varies under the different SRES scenarios (Figure 4c): Under the B1 scenarios, R_h increases at the end of the 21st century, as HC decreases and NPP increases, leaving more biomass to enter the litter pools. Under the A2 and B2 scenarios, however, R_h decreases, as the soil carbon pools decrease. Soil carbon stocks under agricultural land are significantly smaller than under natural forests, although assimilation rates (NPP) do not differ greatly. Larger shares of the assimilated carbon of pastures and cropland are removed at harvest, leaving less litter for decomposition. Under the B2 scenarios, HC decreases after 2020 and NPP levels off around 2060, but the increase of R_h displays a temporal lag because soil carbon stocks are still reduced and accumulate slowly (Figure 4c). Under the A2 scenario, this temporal lag is not perceivable as there is no switch from deforestation to afforestation or vice versa. Wildfire emissions occur in natural forests only and decrease by 1.2 (B2) to 2.4 (A2) PgC/a as the area of natural forests declines, while they remain roughly constant for B1 (Table 3).

The deforestation and afforestation patterns differ regionally, which is also reflected in carbon dynamics. The response of NEE varies, however, as land-use change can both increase or decrease NPP and R_h (Figure 6 g,h,i).

3.3 Combined effects of changes in climate, atmospheric CO_2 concentrations and land use

The terrestrial biosphere is a carbon source throughout the scenario period under the A2 scenarios. Under the B1 and B2 scenarios, the land acts as a net carbon sink after the late 2020s (B1) and the 2040s and 2050s (B2) (Figure 5a). Nonetheless, terrestrial carbon stocks in 2100 are lower relative to 1970 under most scenarios (Figure 3a). They decline under the A2 (-279 to -203 PgC) and B2 (-88 to -40 PgC) scenarios, while they just recover to 1970 levels by 2100 under the B1 scenarios (-4 to 33 PgC). Vegetation carbon decreases under all scenarios, most pronounced under the A2 scenarios where up to 42% of the initial carbon stock is lost by 2100. Soil carbon stocks remain largely unaltered, decreasing slightly under the A2 scenarios and slightly increasing under the B1 and B2 scenarios (Figure 3a).

The increases in NPP caused by climate change and CO_2 fertilization outweigh the small reductions of NPP caused by land-use change, resulting in a net increase of NPP by -10 to -25 PgC/a under all scenarios (Figure 4a, see Table 3 for an overview of NPP, R_h, HC, wildfire emissions, vegetation carbon, and soil carbon). R_h increases in response to the combined effects of changes in climate, atmospheric CO_2 concentrations, and land-use (Figure 4a), even though soil carbon stocks decrease under the A2 scenarios. This is due to rising temperatures and increased input of slash wood into the litter pool. Since most of the deforestation takes place in tropical regions, these additional inputs are respired quickly and thus contribute to the soil respiration flux but do not significantly increase the soil carbon pools. Soil carbon pools decline due to higher carbon exports from harvest (HC). HC in the 21st century corresponds to the development of total cultivated area, i.e. a constant increase for the A2, roughly constant values for the B2 and decreasing values for the B1 scenarios (Figures 1, 5a). Wildfire emissions increase from 3.7 in 1970 to 4.7 and 4.0 PgC/a by 2100 under the B1 and B2 scenarios respectively and decrease to 3.1 PgC/a under the A2 scenarios.

Here, the climate and CO_2 induced increase in litter load is partly compensated (B1) and overcompensated (A2) by land-use change effects on the litter load and the reduction of natural forests. Land-use change effects dominate the resulting NEE of the 21st century (Figure 5a). The land-use change induced carbon losses under the A2 scenarios and also during the first decades under the B1 and B2 scenarios outweigh the climate change and CO_2 fertilization induced terrestrial carbon uptake.

Under the A2 scenarios, land-use change strongly affects the spatial patterns of NEE, especially in North- and South America, but also in Eurasia, Central Africa, and Southeast Asia (Figure 6a,d,g). Under the B1 and B2 scenarios, the spatial patterns of NEE (Figure 6b,c) are dominated by the changes in climate and CO_2 fertilization (Figures 6e,f). As an example of the spatial differences between the four different implementations of each SRES scenario, the standard deviation of the changes in NEE (see Figure 6) are shown in Figure 7 for the combined effects of changes in climate, atmospheric CO_2 concentrations, and land use.

4 Discussion

The 21st century carbon cycle strongly reacts to the projected changes in climate, atmospheric CO_2 concentrations, and land-use. In our simulations, land-use change exerts a strong control on the projected changes in the terrestrial carbon balance during the 21st century, especially under scenarios with high deforestation. The results of our study (covering a range of climatic and socio-economic scenarios) agree with the conclusion of Levy et al. [2004a] that for terrestrial productivity (NPP), land-use change plays a minor role compared to CO_2 fertilization and climatic change. For carbon stocks and the net carbon exchange (NEE), on the contrary, we find that land-use change may well be more important than climatic change, which corresponds well to the findings of Gitz and Ciais [2004], Cramer et al. [2004] (for the tropics only), and Müller et al. [2006].

Land use constitutes a shortcut in the terrestrial carbon cycle. The soil carbon pools are mainly bypassed due to the removal of carbon at harvest and the residence time in the vegetation carbon pools is constrained to less than one year under agriculture. Consequently, large parts of agricultural NPP are directly removed from the terrestrial biosphere, reducing its capacity to sequester carbon (land-use amplifier, see Gitz and Ciais [2003]). On the other hand, land use reduces the terrestrial biosphere's response to climate change: Smaller soil and vegetation carbon stocks only allow for smaller responses to climate change, as there is for example less carbon available for soil respiration.

Still, future terrestrial carbon dynamics remain highly uncertain. Levy et al. [2004a] and Sitch et al. [2005] report only small carbon fluxes due to land-cover and land-use changes that only marginally affect the terrestrial carbon balance. Our results support the findings of Gitz and Ciais [2004] and Cramer et al. [2004], who find land-cover changes to significantly affect the terrestrial carbon budget of the 21st century.

These results, however, cannot be directly compared, as input data used and model assumptions differ considerably. Currently remaining uncertainties in model projections mainly derive from (i) lack of reliable data and consistent definitions of land-use types, (ii) insufficient process-understanding, especially concerning the effects of different management types on the carbon cycle [Liebig et al., 2005], and (iii) the resulting deficiencies in model implementations. Based on the disagreements between the different studies' results as well as observations, we discuss these aspects in the following.

Our land-use flux simulations of the late 20th century compare well to those computed by Houghton [2003] (Figure 8). However, we do not simulate a biospheric carbon sink [Schimel et al., 2001; Bopp et al., 2002; Plattner et al., 2002] during this period. There are two possible reasons for the observed disagreement: (i) the applied rates of land-use change and corresponding carbon fluxes may be overestimated and/or (ii) the residual sink (without land-use change) as computed by LPJmL may be too small.

4.1 Uncertainties in land-use data

The net rate of deforestation (or expansion of cultivated area) in the late 20th century is not well determined and differs considerably between different data sources, a difference that strongly affects the terrestrial carbon balance [Jain and Yang, 2005]. In our study, the expansion of area under cultivation is comparable to the net deforestation rates of 0.13 (1980s) and 0.12 (1990s) million km²/a as reported by Houghton [2003]. Bondeau et al. [2007] compute with LPJmL much smaller carbon emissions from land-use change for the late 20th century, using a land-use data-set with very small deforestation rates of 0.01 million km²/a (based on Ramankutty and Foley [1999] and the HYDE data-base [Klein Goldewijk, 2001]). However, they reproduce the reported small biospheric carbon sink in the 1980s, which increases to approximately -1.1 PgC/a in the 1990s [Schimel et al., 2001; Bopp et al., 2002; Plattner et al., 2002].

Nonetheless, the very small rate of land-use change as reported by Ramankutty and Foley [1999] seems to be unrealistically small. The rates of land-use change under the IMAGE scenarios and as reported by Houghton [2003], on the other hand, may well be too large, considering satellite-observed global deforestation rates of 0.06 (1980s) and 0.07 million km²/a (1990s) [Hansen and DeFries, 2004] that mainly reflect tropical deforestation [Mayaux et al., 2005]. However, when halving the rate of land-use change in our scenarios and the corresponding land-use emissions, the biosphere in our simulations still is a small carbon source or about neutral, suggesting that the residual sink as simulated by LPJmL may also be too small.

4.2 Modeling carbon dynamics under land-use change

The residual sink is determined by the vegetation's response to elevated atmospheric CO_2 concentrations, climate change, and changes in agricultural and forestry management. Possible photosynthetic downregulation under elevated atmospheric CO_2 concentrations is not explicitly considered in LPJmL. The relevant processes are not well understood, especially at the global scale. If there was a significant global effect, the residual sink would be even smaller. However, El Maayar et al. [2006] found photosynthetic downregulation as proposed by Sharkey [1985] to be of minor importance for global NPP. The carbon dynamics of LPJmL under natural vegetation have been compared to atmospheric data [Scholze et al., 2003; Sitch et al., 2003; Peylin et al., 2005]. These studies assumed that the terrestrial biosphere consists of natural vegetation only. The model's ability to reproduce atmospheric measurements under these conditions indicates that the effects of land-use change may be inherently included in the model's parameterization. Consequently, the residual sink of natural vegetation will be underestimated if land-use change is explicitly accounted for, as in our study here.

Management, such as intercropping and fertilization, strongly affects the carbon balance of agricultural land. However, many of the relevant processes have not been

implemented in global carbon models so far, as LPJmL, e.g., does not account for nutrient limitations so far. Some processes are not yet fully understood [Lemaire et al., 2005]. For example, changes in processes of carbon decomposition under cultivation [Post and Kwon, 2000], as well as management and especially management changes are unaccounted for in current global model simulations. Accounting for management is greatly hampered by the lack of suitable data sets on management such as grazing intensities, intercropping, and forest management [Heistermann et al., 2006]. Bondeau et al. [2007] show that differences in agricultural management, represented by intercropping and residue management, can modify the land-use emissions by about 0.2 PgC/a and soil carbon stocks by less than 50 PgC.

Besides, global terrestrial biosphere models just recently have seen the beginning of implementing land-use dynamics in very different ways. Sitch et al. [2005] (based on McGuire et al. [2001]) and Levy et al. [2004a] prescribe special carbon allocation schemes for the NPP of natural vegetation as a proxy for harvest and land-management. In our study and the study of Bondeau et al. [2007], land-use change and managed land are simulated mechanistically.

We also account for managed forests and natural regrowth, however, the current version of LPJmL does not fully reproduce managed forest carbon dynamics: Regrowth of forests after clear-cut is slower than in reality, because age-structure and non-linear shifts in forest growth with stand age are not accounted for in the current version of LPJmL. Zaehle [2005a; 2005b] demonstrated that this may lead to a significant underestimation of carbon sequestration in vegetation after reforestation. This also shows in the slow carbon accumulation in our simulations of the B1 and B2 scenarios. For a European case study, Zaehle et al. [2006] and Zaehle et al. [2007] have demonstrated that including these non-linear processes leads to more plausible estimates of the terrestrial carbon balance.

4.3 Terrestrial carbon cycle of the 21st century

Schaphoff et al. [2006] show that climate projections of several GCMs result in a biospheric carbon source by 2050 for a business as usual emission scenario (IS92a), as also reported by Cox et al. [2000]. We find increasing total carbon pools and stable carbon sinks throughout the entire simulation period under climate and CO_2 change only (CC-simulations). These differences can be explained by the differences in the climate scenarios used [Berthelot et al., 2005] but also by the simplified representation of land-use change effects in form of prescribed CO_2 emissions [Schaphoff et al., 2006] and prescribed grassland to represent agricultural areas in the studies of Cox et al. [2000]. The IMAGE-derived mean temperature changes over land of each SRES scenario (see Table 2) are considerably lower than the GCM-derived temperatures of the IS92a emission scenarios (3.7-6.2°C) as used by Schaphoff et al. [2006]. Thus, heterotrophic respiration in our simulations is not reacting as strongly as in the work of Schaphoff et al. [2006] and the terrestrial biosphere remains a carbon sink if land-use change is excluded. In addition, soil respiration is strongly determined by the size of soil carbon pools, which are considerably smaller under cultivation. Our CC-simulations are computed without land-use change after 1970, i.e. with an agricultural area of ~48 million km² (~37% of total land). Consequently, soil carbon pools and heterotrophic respiration are smaller than under natural vegetation only.

This study covers a broad range of socio-economic scenarios and climate projections. The IMAGE 2.2 implementations of the SRES scenarios take into account a broad range of feedbacks and drivers to derive land-use patterns and, thus, this study currently is – to our knowledge – the most comprehensive study on the effects of land-use change on the carbon budget at the global scale. Here, we focused on generally different trends in socio-economic development (SRES scenarios) and uncertainties in climate projections (GCM patterns). Uncertainties in global trade, lifestyle, and technological progress are not addressed here.

This, however, would be desirable since these are important drivers of land-use change and yield the potential to strongly affect the terrestrial carbon balance [Müller et al., 2006].

5 Conclusions

Our simulations have shown that projected land-use change under different socio-economic scenarios have profound effects on the terrestrial carbon balance and potentially offset the effects of climate change. Climate change and CO_2 fertilization cause a net terrestrial carbon uptake of 105-225 PgC over the period 1970-2100, while land use and land-use change cause a net carbon loss of 110 to 445 PgC. CO_2 fertilization and climatic change mainly determine the increase of NPP, while land-use change shows only small effects on NPP. Studies of global change, including studies on the carbon cycle, and climate change need to account for land-use change. The exclusion of land use, which is still common in global biogeochemical modeling, significantly reduces the relevance of future projections of the development of the global carbon cycle and limits the insights gained in these studies.

However, we stress that the inclusion of land use and land-use change into global simulations is currently still hampered significantly by data availability and reliability as well as a corresponding lack of implementation of relevant processes in models. Models need to account for more processes such as a more detailed characterization of land management. Future changes in land-use technology, global dietary life styles or the dynamics of large-scale bioenergy use are partially included in the SRES scenarios. Their dynamics beyond these assumptions will additionally alter the projections of the carbon cycle. Progress in our ability to model these processes should be a priority.

Acknowledgements

CM was supported by the International Max Planck Research School on Earth System Modeling (IMPRS-ESM), Hamburg, Germany, We acknowledge the Commission of the European Communities' project MATISSE (004059-GOCE) and the European Science Foundation (ESF) “The Role of Soils in the Terrestrial Carbon Balance” for financial support. We thank Ben Poulter and anonymous reviewers for helpful comments.

References

Achard, F., H. D. Eva, H.-J. Stibig, P. Mayaux, J. Gallego, T. Richards and J.-P. Malingreau (2002), Determination of Deforestation Rates of the World's Humid Tropical Forests, *Science 297*(5583), 999-1002.

Alcamo, J., R. Leemans and E. Kreileman (Eds.) (1998), *Global Change Scenarios of the 21st Century - Results from the IMAGE 2.1 Model*, Elsevier Science Ldt, Oxford, UK.

Andreae, M. O. and P. Merlet (2001), Emission of trace gases and aerosols from biomass burning, *Global Biogeochem. Cycles 15*(4), 955-966.

Bacher, A., J. M. Oberhuber and E. Roeckner (1998), ENSO dynamics and seasonal cycle in the tropical Pacific as simulated by the ECHAM4/OPYC3 coupled general circulation model, *Climate Dynamics 14*, 431-450.

Beer, C., W. Lucht, C. Schmullius and A. Shvidenko (2006), Small net carbon dioxide uptake by Russian forests during 1981-1999, *Geophys. Res. Lett. 33*, L15403, doi:10.1029/2006GL026919.

Berthelot, M., P. Friedlingstein, P. Ciais, J.-L. Dufresne and P. Monfray (2005), How uncertainties in future climate change predictions translate into future terrestrial carbon fluxes, *Global Change Biol. 11*(6), 959-970.

Boer, G. J., G. M. Flato, M. C. Reader and D. Ramsden (2000), A transient climate change simulation with greenhouse gas and aerosol forcing: experimental design and comparison with the instrumental record for the twentieth century, *Climate Dynamics 16*, 405-425.

Bondeau, A., P. Smith, S. Zaehle, S. Schaphoff, W. Lucht, W. Cramer, D. Gerten, H. Lotze-Campen, C. Müller, M. Reichstein and B. Smith (2007), Modelling the role of agriculture for the 20th century global terrestrial carbon balance, *Global Change Biol. 13*(3), 679-706, doi:10.1111/j.1365-2486.2006.01305.x.

Bopp, L., C. Le Quere, M. Heimann, A. C. Manning and P. Monfray (2002), Climate-induced oceanic oxygen fluxes: Implications for the contemporary carbon budget, *Global Biogeochem. Cycles 16*(2).

Bradford, J. B., W. K. Lauenroth and I. C. Burke (2005), The impact of cropping on primary production in the US great plains, *Ecology 86*(7), 1863-1872.

Canadell, J. (2002), Land use effects on terrestrial carbon sources and sinks, *Science in China Series C-Life Sciences 45*, 1-9 Suppl.

Carter, T. R., M. L. Parry, H. Harasawa and S. Nishioka (1994), IPCC Technical Guidelines for Assessing Impacts of Climate Change, IPCC Special Report 0904813118, Intergovernmental Panel on Climate Change, WMO and UNEP, pp. 59 Geneva.

Caspersen, J., S. Pacala, J. Jenkins, G. Hurtt, P. Moorcroft and R. Birdsey (2000), Contributions of land-use history to carbon accumulation in US forests, *Science 290*(5494), 1148-1151.

Cox, P. M., R. A. Betts, C. D. Jones, S. A. Spall and I. J. Totterdell (2000), Acceleration of global warming due to carbon-cycle feedbacks in a coupled climate model, *Nature 408*(6813), 184-187.

Cramer, W., A. Bondeau, S. Schaphoff, W. Lucht, B. Smith and S. Sitch (2004), Tropical forests and the global carbon cycle: impacts of atmospheric carbon dioxide, climate change and rate of deforestation, *Philos. Trans. R. Soc. London Ser. B 359*(1443), 331-343.

Dargaville, R. J., M. Heimann, A. D. McGuire, I. C. Prentice, D. Kicklighter, F. Joos, J. S. Clein, G. Esser, J. Foley, J. Kaplan, R. A. Meier, J. M. Melillo, B. Moore III, N. Ramankutty, T. Reichenau, A. Schloss, S. Sitch, H. Tian, L. J. Williams and U. Wittenberg (2002), Evaluation of terrestrial carbon cycle models with atmospheric CO_2 measurements: Results from transient simulations considering increasing CO_2, climate,

and land-use effects, *Global Biogeochem. Cycles 16*(4), 1092, doi:10.1029/2001GB001426.

DeFries, R. (2002), Past and future sensitivity of primary production to human modification of the landscape, *Geophys. Res. Lett. 29*(7), 36-1-36-4.

Dufresne, J.-L., P. Friedlingstein, M. Berthelot, L. Bopp, P. Ciais, L. Fairhead, H. Le Treut and P. Monfray (2002), On the magnitude of positive feddback between future climate change and the carbon cycle, *Geophys. Res. Lett. 29*(10), 1405, doi:10.1029/2001GL013777.

El Maayar, M., N. Ramankutty and C. J. Kucharik (2006), Modeling Global and Regional Net Primary Production under Elevated Atmospheric CO_2: On a Potential Source of Uncertainty, *Earth Interactions 10*(Paper No. 2).

FAOSTAT data (2005), http://faostat.fao.org/ [Accessed: March, 2005].

Fearnside, P. M. (2000), Global warming and tropical land-use change: Greenhouse gas emissions from biomass burning, decomposition and soils in forest conversion, shifting cultivation and secondary vegetation, *Climatic Change 46*(1-2), 115-158.

Foley, J., R. DeFries, G. P. Asner, C. Barford, G. Bonan, S. R. Carpenter, F. S. Chapin, M. T. Coe, G. C. Daily, H. K. Gibbs, J. H. Helkowski, T. Holloway, E. A. Howard, C. J. Kucharik, C. Monfreda, J. A. Patz, I. C. Prentice, N. Ramankutty and P. K. Snyder (2005), Global Consequences of Land Use, *Science 309*(5734), 570-574.

Friedlingstein, P., J. Dufresne, P. Cox and P. Rayner (2003), How positive is the feedback between climate change and the carbon cycle?, *Tellus Series B-Chemical and Physical Meteorology 55*(2), 692-700.

Gerten, D., S. Schaphoff, U. Haberlandt, W. Lucht and S. Sitch (2004), Terrestrial vegetation and water balance - hydrological evaluation of a dynamic global vegetation model, *Journal of Hydrology 286*(1-4), 249-270.

Gerten, D., W. Lucht, S. Schaphoff, W. Cramer, T. Hickler and W. Wagner (2005), Hydrologic resilience of the terrestrial biosphere, *Geophys. Res. Lett. 32*(21).

Gitz, V. and P. Ciais (2003), Amplifying effects of land-use change on future atmospheric CO_2 levels, *Global Biogeochem. Cycles 17*(1), 1024, doi:10.1029/2002GB001963.

Gitz, V. and P. Ciais (2004), Future Expansion Of Agriculture and Pasture Acts to Amplify Atmospheric CO_2 Levels in Response to Fossil-Fuel and Land-Use Change Emissions, *Climatic Change 67*(2), 161-184.

Guo, L. B. and R. M. Gifford (2002), Soil carbon stocks and land use change: a meta analysis, *Global Change Biol. 8*(4), 345-360.

Haberl, H., K. H. Erb, F. Krausmann, W. Loibl, N. Schulz and H. Weisz (2001), Changes in ecosystem processes induced by land use: Human appropriation of aboveground NPP and its influence on standing crop in Austria, *Global Biogeochem. Cycles 15*(4), 929-942.

Hansen, M. C. and R. S. DeFries (2004), Detecting Long-term Global Forest Change Using Continuous Fields of Tree-Cover Maps from 8-km Advanced Very High Resolution Radiometer (AVHRR) Data for the Years 1982-99, *Ecosystems 7*(7), 695-716.

Heistermann, M., C. Müller and K. Ronneberger (2006), Land in sight? Achievements, deficits and potentials of global land-use modeling, *Agriculture Ecosystems & Environment 114*(2-4), 141-158, doi:10.1016/j.agee.2005.11.015.

Hirst, A. C., H. B. Gordon and S. P. O' Farrell (1996), Global warming in a coupled climate model including oceanic eddy-induced advection, *Geophys. Res. Lett. 23*, 3361-3364.

Houghton, R. (2003), Revised estimates of the annual net flux of carbon to the atmosphere from changes in land use and land management 1850-2000, *Tellus Series B-Chemical and Physical Meteorology 55*(2), 378-390.

Houghton, R. A. (1999), The annual net flux of carbon to the atmosphere from changes in land use 1850-1990, *Tellus Series B-Chemical and Physical Meteorology 51*(2), 298-313.

House, J. I., I. C. Prentice and C. Le Quere (2002), Maximum impacts of future reforestation or deforestation on atmospheric CO_2, *Global Change Biol. 8*(11), 1047-1052.

IMAGE team (2001), The IMAGE 2.2 implementation of the SRES scenarios: A comprehensive analysis of emissions, climate change and impacts in the 21st century, National Institute for Public Health and the Environment, RIVM CD-ROM publication 481508018 Bilthoven, The Netherlands.

Jain, A. K. and X. Yang (2005), Modeling the effects of two different land cover change data sets on the carbon stocks of plants and soils in concert with CO2 and climate change, *Global Biogeochem. Cycles 19*(GB2015), doi:10.1029/2004GB002349.

Jones, M. B. and A. Donnelly (2004), Carbon sequestration in temperate grassland ecosystems and the influence of management, climate and elevated CO2, *New Phytol. 164*(3), 423-439.

Keeling, C. D. and T. P. Whorf (2003), Atmospheric CO_2 records from sites in the SIO air sampling network. In Trends: A Compendium of Data on Global Change. Carbon Dioxide Information Analysis Center, Oak Ridge National Laboratory, U.S. Department of Energy Oak Ridge, Tenn., U.S.A.

Klein Goldewijk, K. (2001), Estimating global land use change over the past 300 years: The HYDE Database, *Global Biogeochem. Cycles 15*(4), 417-433.

Lal, R. (2004), Soil Carbon Sequestration Impacts on Global Climate Change and Food Security, *Science 304*(5677), 1623-1627.

Lambin, E. F., B. L. Turner, H. J. Geist, S. B. Agbola, A. Angelsen, J. W. Bruce, O. T. Coomes, R. Dirzo, G. Fischer, C. Folke, P. S. George, K. Homewood, J. Imbernon, R. Leemans, X. B. Li, E. F. Moran, M. Mortimore, P. S. Ramakrishnan, J. F. Richards, H. Skanes, W. Steffen, G. D. Stone, U. Svedin, T. A. Veldkamp, C. Vogel and J. C. Xu (2001), The causes of land-use and land-cover change: moving beyond the myths, *Global Environmental Change - Human and Policy Dimensions 11*(4), 261-269.

Leemans, R., B. Eickhout, B. Strengers, L. Bouwman and M. Schaeffer (2002), The consequences of uncertainties in land use, climate and vegetation responses on the terrestrial carbon, *Science in China Series C-Life Sciences 45*, 126+ Suppl. S.

Lemaire, G., R. Wilkins and J. Hodgson (2005), Challenges for grassland science: managing research priorities, *Agriculture, Ecosystems & Environment 108*(2), 99-108.

Levy, P., M. Cannell and A. Friend (2004a), Modelling the impact of future changes in climate, CO_2 concentration and land use on natural ecosystems and the terrestrial carbon sink, *Global Environmental Change - Human and Policy Dimensions 14*(1), 21-20.

Levy, P. E., A. D. Friend, A. White and M. G. R. Cannell (2004b), The Influence of Land Use Change On Global-Scale Fluxes of Carbon from Terrestrial Ecosystems, *Climatic Change 67*(2), 185-209.

Liebig, M. A., J. A. Morgan, J. D. Reeder, B. H. Ellert, H. T. Gollany and G. E. Schuman (2005), Greenhouse gas contributions and mitigation potential of agricultural practices in northwestern USA and western Canada, *Soil & Tillage Research 83*, 25-52.

Lohila, A., M. Aurela, J.-P. Tuovinen and T. Laurila (2004), Annual CO2 exchange of a peat field growing spring barley or perennial forage grass, *J. Geophys. Res. 109*, D18116, doi:10.1029/2004JD004715.

Lucht, W., I. C. Prentice, R. B. Myneni, S. Sitch, P. Friedlingstein, W. Cramer, P. Bousquet, W. Buermann and B. Smith (2002), Climatic Control of the High-Latitude Vegetation Greening Trend and Pinatubo Effect, *Science 296*(5573), 1687-1689.

Matthews, H. D., A. J. Weaver and K. J. Meissner (2005), Terrestrial Carbon Cycle Dynamics under Recent and Future Climate Change, *Journal of Climate 18*(10), 1609-1628.

Mayaux, P., P. Holmgren, F. Achard, H. Eva, H. Stibig and A. Branthomme (2005), Tropical forest cover change in the 1990s and options for future monitoring, *Philosophical Transactions of the Royal Society B-Biological Sciences 360*(1454), 373-384.

McGuire, A., S. Sitch, J. Clein, R. Dargaville, G. Esser, J. Foley, M. Heimann, F. Joos, J. Kaplan, D. Kicklighter, R. Meier, J. Melillo, B. Moore, I. Prentice, N. Ramankutty, T. Reichenau, A. Schloss, H. Tian, L. Williams and U. Wittenberg (2001), Carbon balance of the terrestrial biosphere in the twentieth century: Analyses of CO_2, climate and land use effects with four process-based ecosystem models, *Global Biogeochem. Cycles 15*(1), 183-206.

Mitchell, J. F. B., T. C. Johns, J. M. Gregory and S. F. B. Tett (1995), Climate response to increasing levels of greenhouse gases and sulphate aerosols, *Nature 376*, 501-504.

Mitchell, T. D., T. R. Carter, P. D. Jones, M. Hulme and M. New (2004), A comprehensive set of high-resolution grids of monthly climate for Europe and the globe: The observed record (1901-2000) and 16 scenarios (2001-2100), Technical report, no. 5, Tyndall Centre for Climate Change Research, University of East Anglia Norwich, UK.

Müller, C., A. Bondeau, H. Lotze-Campen, W. Lucht and W. Cramer (2006), Comparative impact of climatic and nonclimatic factors on global terrestrial carbon and water cycles, *Global Biogeochem. Cycles 20*, GB4015, doi:10.1029/2006GB002742.

Murphy, J. M., D. M. H. Sexton, D. N. Barnett, G. S. Jones, M. J. Webb, M. Collins and D. A. Stainforth (2004), Quantification of modelling uncertainties in a large ensemble of climate change simulations, *Nature 430*(7001), 768-772.

Myneni, R. B., R. R. Nemani and S. W. Running (1997), Estimation of Global Leaf Area Index and Absorbed Par Using Radiative Transfer Models, *IEEE Transactions on Geoscience and Remote Sensing 35*(6), 1380-1393.

Nakicenovic, N. and R. Swart (Eds.) (2000), *Special Report on Emisson Scenarios*, 599 pp., Cambridge University Press, Cambrige, UK.

Ometto, J., A. Nobre, H. Rocha, P. Artaxo and L. Martinelli (2005), Amazonia and the modern carbon cycle: lessons learned, *Oecologia 143*(4), 483-500.

Peylin, P., P. Bousquet, C. Le Quéré, S. Sitch, P. Friedlingstein, G. McKinley, N. Gruber, P. Rayner and P. Ciais (2005), Multiple constraints on regional CO_2 flux variations over land and oceans, *Global Biogeochem. Cycles 19*, GB1011, doi:10.1029/2003GB002214.

Plattner, G. K., F. Joos and T. F. Stocker (2002), Revision of the global carbon budget due to changing air-sea oxygen fluxes, *Global Biogeochem. Cycles 16*(4).

Post, W. and K. Kwon (2000), Soil carbon sequestration and land-use change: processes and potential, *Global Change Biol. 6*(3), 317-327.

Ramankutty, N. and J. Foley (1999), Estimating historical changes in global land cover: Croplands from 1700 to 1992, *Global Biogeochem. Cycles 13*(4), 997-1027.

Schaphoff, S., W. Lucht, D. Gerten, S. Sitch, W. Cramer and I. C. Prentice (2006), Terrestrial biosphere carbon storage under alternative climate projections, *Climatic Change*, doi:10.1007/s10584-005-9002-5.

Schimel, D., J. House, K. Hibbard, P. Bousquet, P. Ciais, P. Peylin, B. Braswell, M. Apps, D. Baker, A. Bondeau, J. Canadell, G. Churkina, W. Cramer, A. Denning, C. Field, P. Friedlingstein, C. Goodale, M. Heimann, R. Houghton, J. Melillo, B. Moore, D. Murdiyarso, I. Noble, S. Pacala, I. Prentice, M. Raupach, P. Rayner, R. Scholes, W. Steffen and C. Wirth (2001), Recent patterns and mechanisms of carbon exchange by terrestrial ecosystems, *Nature 414*(6860), 169-172.

Schlesinger, M. E., S. Malyshev, E. V. Rozanov, F. Yang, N. G. Andronova, B. de Vries, A. Grübler, K. Jiang, T. Masui, T. Morita, N. Nakicenovic, J. Penner, W. Pepper, A. Sankovski and Y. Zhang (2000), Geographical distributions of temperature change for scenarios of greenhouse gas and sulfur dioxide emissions, *Technological Forecasting and Social Change 65*, 167-193.

Scholze, M., J. Kaplan, W. Knorr and M. Heimann (2003), Climate and interannual variability of the atmosphere-biosphere $^{13}CO_2$ flux, *Geophys. Res. Lett. 30*(2), doi:10.1029/2002GL015631.

Schröter, D., W. Cramer, R. Leemans, I. C. Prentice, M. B. Araujo, N. W. Arnell, A. Bondeau, H. Bugmann, T. R. Carter, C. A. Gracia, A. C. de la Vega-Leinert, M. Erhard, F. Ewert, M. Glendining, J. I. House, S. Kankaanpaa, R. J. T. Klein, S. Lavorel, M. Lindner, M. J. Metzger, J. Meyer, T. D. Mitchell, I. Reginster, M. Rounsevell, S. Sabate, S. Sitch, B. Smith, J. Smith, P. Smith, M. T. Sykes, K. Thonicke, W. Thuiller, G. Tuck, S. Zaehle and B. Zierl (2005), Ecosystem Service Supply and Vulnerability to Global Change in Europe, *Science 310*(5752), 1333-1337.

Sharkey, T. D. (1985), Photosynthesis in Intact Leaves of C-3 Plants - Physics, Physiology and Rate Limitations, *Botanical Review 51*(1), 53-105.

Sitch, S., V. Brovkin, W. von Bloh, D. van Vuuren, B. Eickhout and A. Ganopolski (2005), Impacts of future land cover changes on atmospheric CO_2 and climate., *Global Biogeochem. Cycles 19*(GB2013), doi:10.1029/2004GB002311.

Sitch, S., B. Smith, I. Prentice, A. Arneth, A. Bondeau, W. Cramer, J. Kaplan, S. Levis, W. Lucht, M. Sykes, K. Thonicke and S. Venevsky (2003), Evaluation of ecosystem dynamics, plant geography and terrestrial carbon cycling in the LPJ dynamic global vegetation model, *Global Change Biol. 9*(2), 161-185.

Smith, J., P. Smith, M. Wattenbach, S. Zaehle, R. Hiederer, R. J. A. Jones, L. Montanarella, M. D. A. Rounsevell, I. Reginster and F. Ewert (2005), Projected changes in mineral soil carbon of European croplands and grasslands, 1990-2080, *Global Change Biol. 11*(12), 2141-2152.

Smith, P., J. Smith, M. Wattenbach, M. Meyer, M. Lindner, S. Zaehle, R. Hiederer, R. Jones, L. Montanarella, M. D. A. Rounsevell and I. Reginster (2006), Projected changes in mineral soil carbon of European forests,

1990-2100, *Canadian Journal of Soil Science 86*(2), 159-169.

Smith, T. M., W. P. Cramer, R. K. Dixon, R. Leemans, R. P. Neilson and A. M. Solomon (1993), The global terrestrial carbon cycle, *Water, Air, & Soil Pollution 70*(1 - 4), 19-37.

Thonicke, K., S. Venevsky, S. Sitch and W. Cramer (2001), The role of fire disturbance for global vegetation dynamics: coupling fire into a Dynamic Global Vegetation Model, *Global Ecology & Biogeography 10*, 661-677.

USDA (1994), Major World Crop Areas and Climatic Profiles, Agricultural Handbook No. 664, US Department of Agriculture (USDA), World Agricultural Outlook Board, Joint Agricultural Weather Facility Washington, D.C.

Wagner, W., K. Scipal, C. Pathe, D. Gerten, W. Lucht and B. Rudolf (2003), Evaluation of the agreement between the first global remotely sensed soil moisture data with model and precipitation data, *Journal of Geophysical Research-Atmospheres 108*(D19).

Zaehle, S. (2005a), Effect Of Height On Tree Hydraulic Conductance Incompletely Compensated By Xylem Tapering, *Functional Ecology 19*(2), 359-364.

Zaehle, S., 2005b. Process-based simulation of the European terrestrial biosphere (Thesis), 191 pp., Potsdam, Potsdam University.

Zaehle, S., S. Sitch, B. Smith and F. Hatterman (2005), Effects of parameter uncertainties on the modeling of terrestrial biosphere dynamics, *Global Biogeochem. Cycles 19*(GB3020), doi:10.1029/2004GB002395.

Zaehle, S., S. Sitch, I. C. Prentice, J. Liski, W. Cramer, M. Erhard, T. Hickler and B. Smith (2006), The importance of age-related decline of forest NPP for modeling regional carbon balances, *Ecological Applications 16*(4).

Zaehle, S., A. Bondeau, T. Carter, W. Cramer, M. Erhard, I. C. Prentice, I. Reginster, M. Rounsevell, S. Sitch, B. Smith, P. Smith and M. T. Sykes (2007), Projected changes in terrestrial carbon storage in Europe under climate and land-use change, 1990-2100, *Ecosystems*, doi: 10.1007/s10021-007-9028-9.

Table 1. Mapping of IMAGE land-use classes to LPJmL categries and CFTs.

IMAGE land-use class	LPJmL representation
Grassland (rain-fed)	C3 or C4 grass, depending on suitability as determined by LPLmL (default: C4 in the tropics, else C3)
Temperate cereals (rain-fed)	Temperate cereals (rain-fed)
Rice (rain-fed)	Rice (rain-fed)
Maize (rain-fed)	Maize (rain-fed)
Tropical cereals (rain-fed)	Tropical cereals (rain-fed)
Pulses (rain-fed)	Pulses (rain-fed)
Roots and tubers (rain-fed)	Rain-fed temperate (Sugar beet) or tropical (Manioc) roots and tubers, depending on LPJmL-suitability. Default setting: Manioc in the tropics, else Sugar beets
Oil crops (rain-fed)	Rain-fed soybeans, peanuts, sunflowers or rapeseed, depending on LPJmL-suitability. Default setting: soybeans in the tropics, else rapeseed
Temperate cereals (irrigated)	Temperate Cereals (irrigated)
Rice (irrigated)	Rice (irrigated)
Maize (irrigated)	Maize (irrigated)
Tropical cereals (irrigated)	Tropical Cereals (irrigated)
Pulses (irrigated)	Pulses (irrigated)
Roots and tubers (irrigated)	Irrigated temperate (Sugar beet) or tropical (Manioc) roots and tubers, depending on LPJmL-suitability. Default setting: Manioc in the tropics, else Sugar beets
Oil crops (irrigated)	Irrigated soybeans, peanuts, sunflowers or rapeseed, depending on LPJmL-suitability. Default setting: soybeans in the tropics, else rapeseed
Sugar cane (biofuel, rain-fed)	Maize (rain-fed)
Maize (biofuel)	Maize (rain-fed)
Non-woody biofuels (biofuel, rain-fed)	C3 or C4 grass, depending on suitability as determined by LPLmL (default: C4 in the tropics, else C3)
Woody biofuels (biofuel, rain-fed)	No CFT assigned but treated as managed forest
Timber	Managed forest
Regrowth	Natural vegetation (composition internally determined by LPJmL)
Natural land-cover classes	Natural vegetation (composition internally determined by LPJmL)

Table 2. Scenario characteristics as supplied by IMAGE 2.2 [IMAGE team, 2001].

Temperature changes are computed as the difference between the 1971-2000 and 2071-2100 averages over land.

Scenario SRES	GCM pattern	Atmospheric [CO_2] in 2100 [ppm]	Temperature increase 1970-2100 [°C]	Land area changes 1970-2100 [mill. km²]		
				Cropland	Managed Grassland	Managed Forest
A2	CGCM	865.7	3.4	17.02	4.17	4.08
	CSIRO	847.8	3.1	16.34	2.56	4.00
	ECHAM	859.5	3.8	17.51	3.91	4.06
	HADCM	863.3	3.5	16.69	3.90	4.24
B1	CGCM	521.7	2.2	1.02	-11.31	3.09
	CSIRO	514.6	2.1	0.93	-11.67	3.02
	ECHAM	518.3	2.4	1.01	-11.55	3.00
	HADCM	517.8	2.2	1.03	-11.53	2.96
B2	CGCM	609.6	2.7	7.09	-4.68	4.19
	CSIRO	599.7	2.6	6.79	-5.38	4.26
	ECHAM	605.6	3.1	7.26	-5.24	4.20
	HADCM	604.7	2.8	7.15	-4.91	4.23

Table 3: Selected results of the CC and CCL simulations.

Scenario		NPP [PgC/a]		R_h [PgC/a]		HC [PgC/a]		Wildfire emissions [PgC/a]		Vegetation carbon [PgC]		Soil carbon [PgC]	
SRES	GCM pattern	1970-1979	2091-2100	1970-1979	2091-2100	1970-1979	2091-2100	1970-1979	2091-2100	1970-1979	2091-2100	1970-1979	2091-2100
						CC simulations							
	HADCM		75.8		51.4		17.5		5.3		703		1047
	ECHAM		77.1		52.2		17.8		5.7		706		1035
A2	CGCM	54.5	77.0	36.5	51.9	13.7	17.5	3.8	5.8	599	710	993	1067
	CSIRO		80.7		54.4		18.5		5.4		734		1070
	average		77.7		52.5		17.8		5.5		713		1055
	HADCM		64.1		43.6		15.0		4.9		677		1020
	ECHAM		64.8		44.0		15.2		5.1		676		1016
B1	CGCM	54.5	64.6	36.5	43.9	13.7	14.9	3.8	5.1	599	676	993	1036
	CSIRO		66.4		45.2		15.4		4.9		691		1038
	average		65.0		44.2		15.1		5.0		680		1027
	HADCM		67.5		45.9		15.6		5.0		683		1024
	ECHAM		68.4		46.4		15.9		5.3		683		1018
B2	CGCM	54.5	68.2	36.5	46.3	13.7	15.5	3.8	5.3	599	685	993	1042
	CSIRO		70.8		48.0		16.3		5.1		703		1044
	average		68.7		46.6		15.8		5.2		689		1032
						CCL simulations							
	HADCM		71.7		41.9		30.0		2.9		368		973
	ECHAM		73.5		43.2		30.8		3.1		367		961
A2	CGCM	54.3	73.0	36.5	42.4	15.3	30.5	3.7	3.1	589	368	992	989
	CSIRO		76.6		45.2		30.6		3.1		403		994
	average		73.7		43.2		30.5		3.1		377		979
	HADCM		63.2		44.4		12.4		4.6		551		1029
	ECHAM		64.0		44.9		12.5		4.8		551		1026
B1	CGCM	54.3	63.8	36.5	44.6	15.3	12.5	3.7	4.7	589	547	992	1044
	CSIRO		65.4		45.9		12.7		4.7		565		1047
	average		64.1		45.0		12.5		4.7		553		1037
	HADCM		65.4		42.7		17.7		3.8		503		1002
	ECHAM		66.7		43.5		18.0		4.1		501		996
B2	CGCM	54.3	66.4	36.5	43.2	15.3	17.9	3.7	4.0	589	500	992	1018
	CSIRO		68.8		44.9		18.3		4.0		520		1021
	average		66.8		43.6		18.0		4.0		506		1009

Figures:

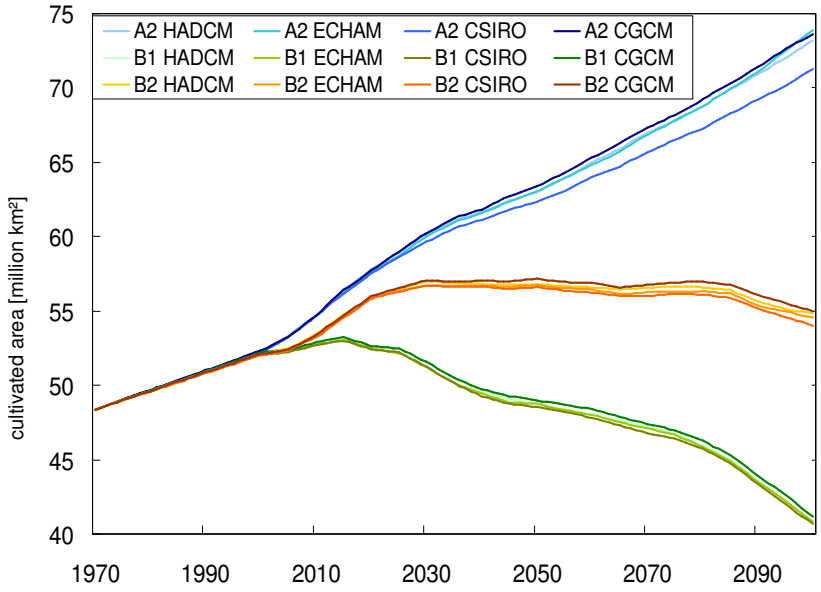

Figure 1. Temporal development of global total cultivated area (cropland, pasture, and managed forests) for the 12 scenarios.

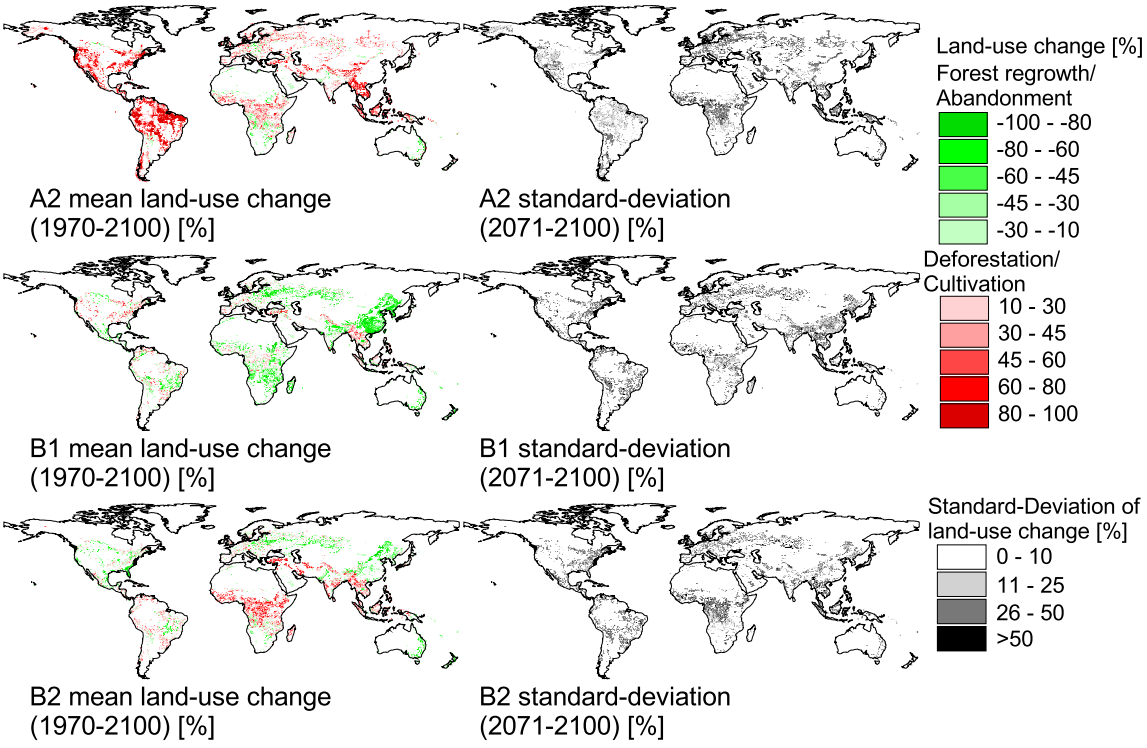

Figure 2. Mean land-use change from 1970 to 2100 for the SRES scenarios A2, B1 and B2, averaged over the 4 data sets for each scenario (see section 2.2). The difference (0.5x0.5°) between these is shown on the right as the standard deviation, the regional differences, however, are very small.

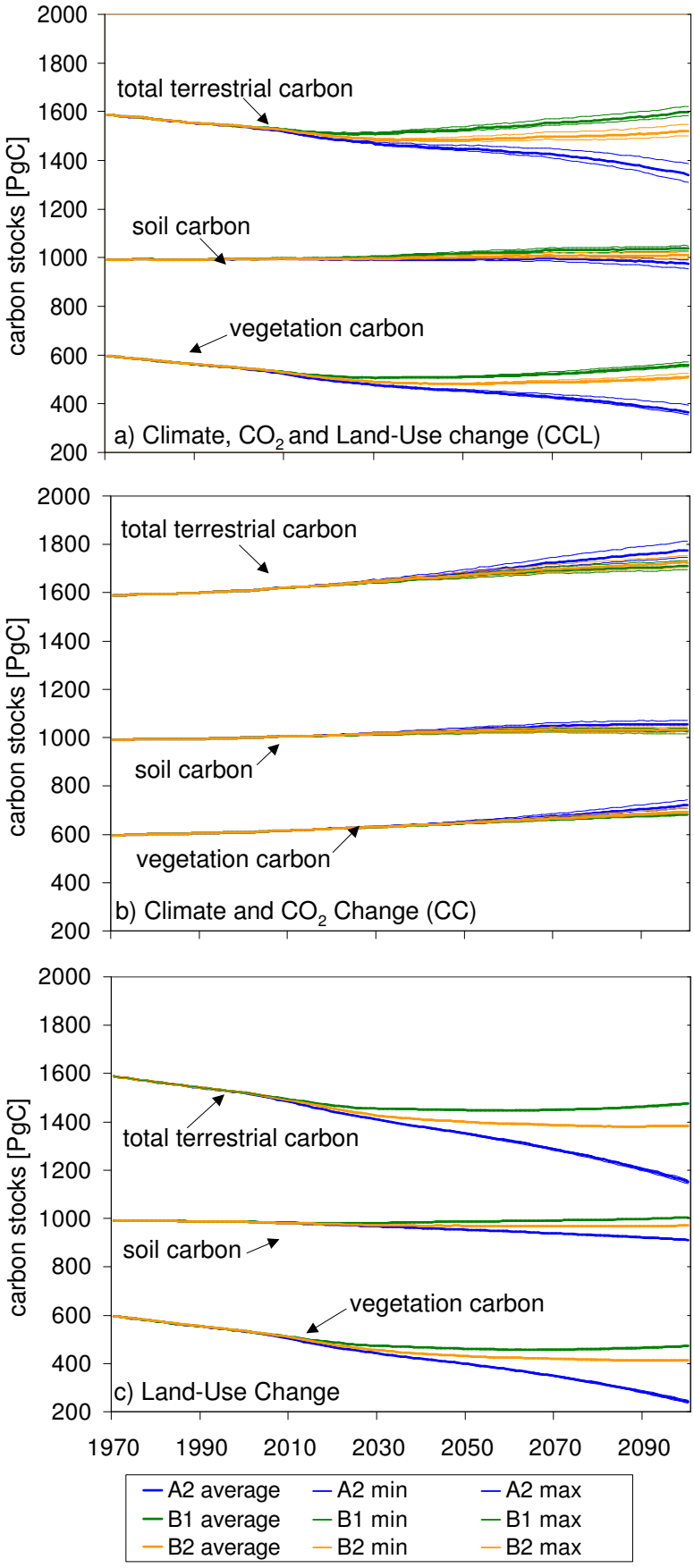

Figure 3. Terrestrial carbon stocks. Bold lines represent the average for each SRES scenario; thin lines represent the min/max range. Panel c) represents the difference of a) and b) added to the initial value of 1970, in order to obtain the same scale in panels a)-c).

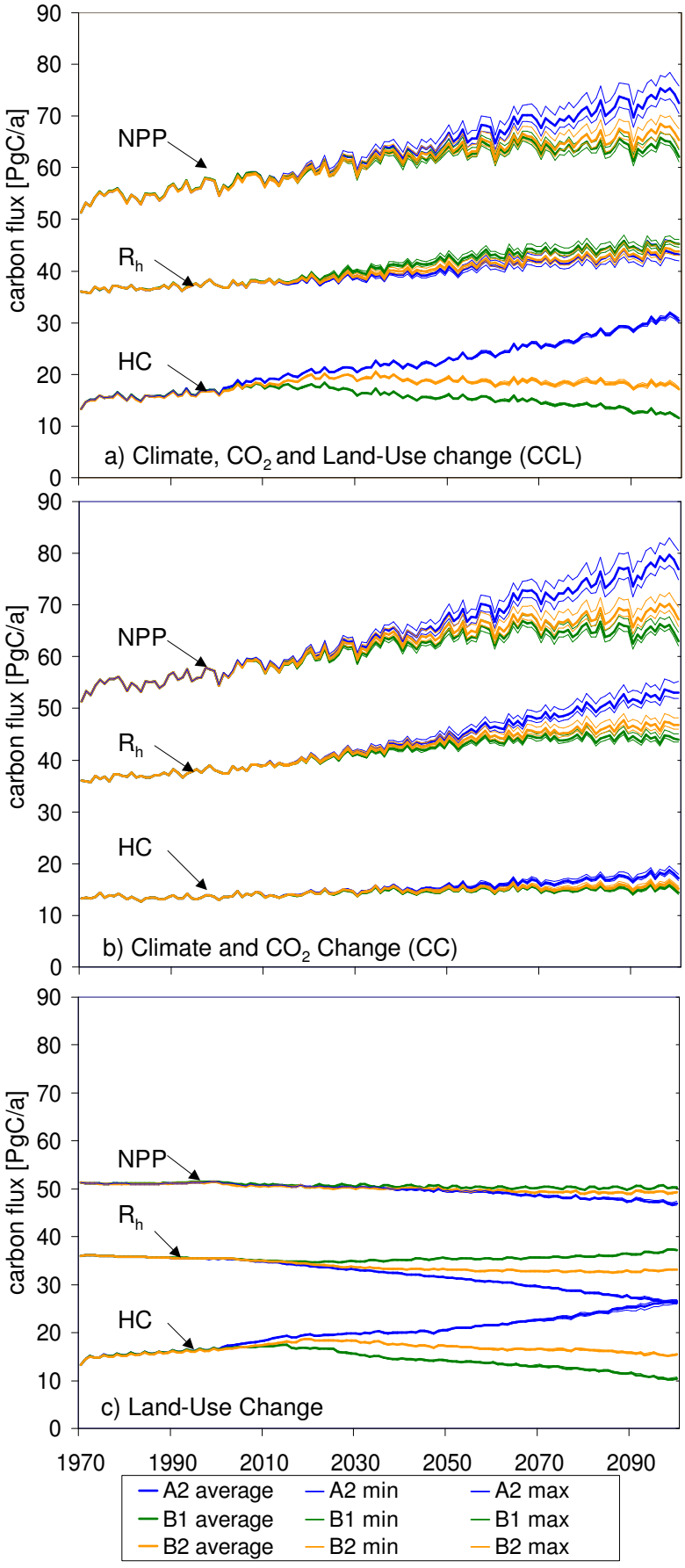

Figure 4. Carbon fluxes. Bold lines represent the average for each SRES scenario; thin lines represent the min/max range. Fire emissions (< 6 PgC/a) are not shown. Note that R_h and HC represent carbon fluxes from the biosphere to the atmosphere. Panel c) represents the difference of a) and b) added to the initial value of 1970, in order to obtain the same scale in panels a)-c).

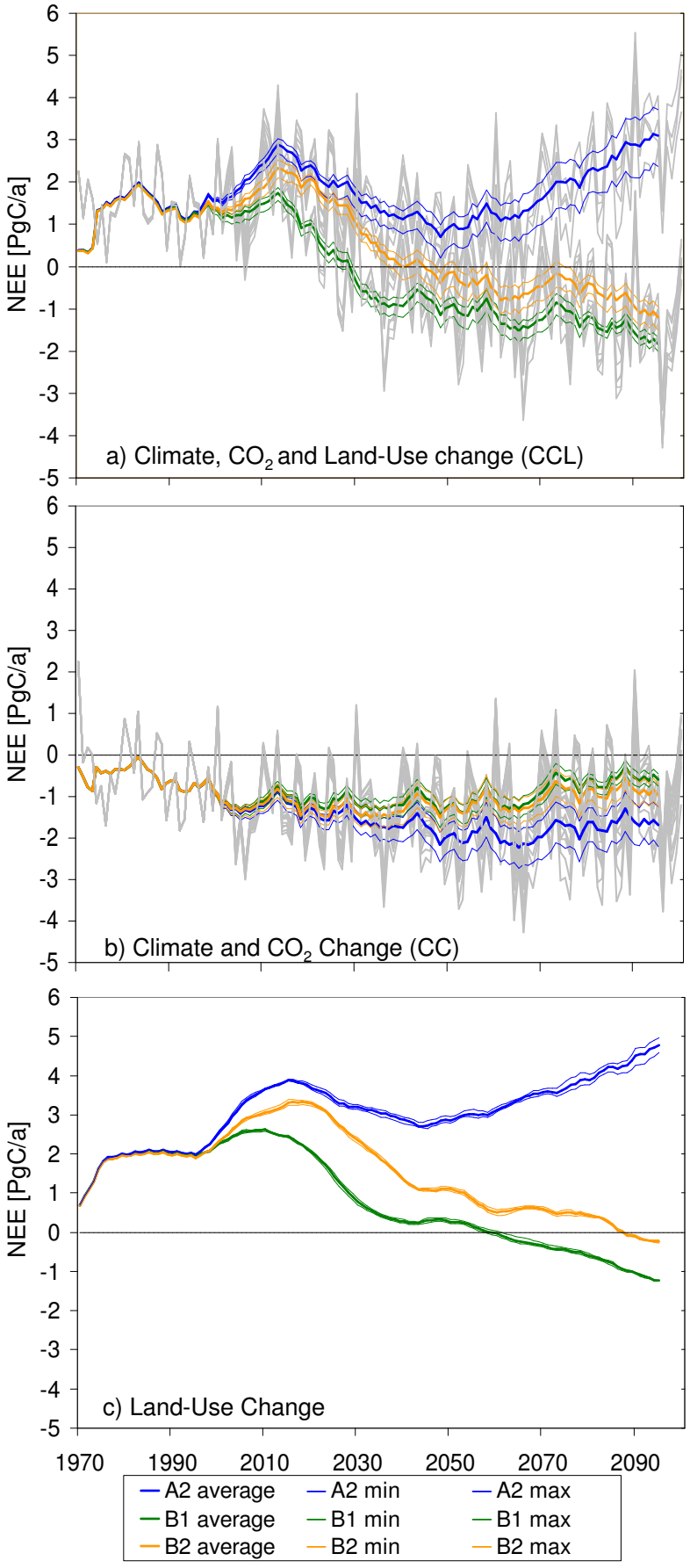

Figure 5. Net ecosystem exchange (10-year running mean). Bold lines represent the average for each SRES scenario; thin lines represent the min/max range; grey lines represent the annual fluctuations. Negative values indicate a carbon flux from the atmosphere to the biosphere. Panel c) represents the difference of a) and b).

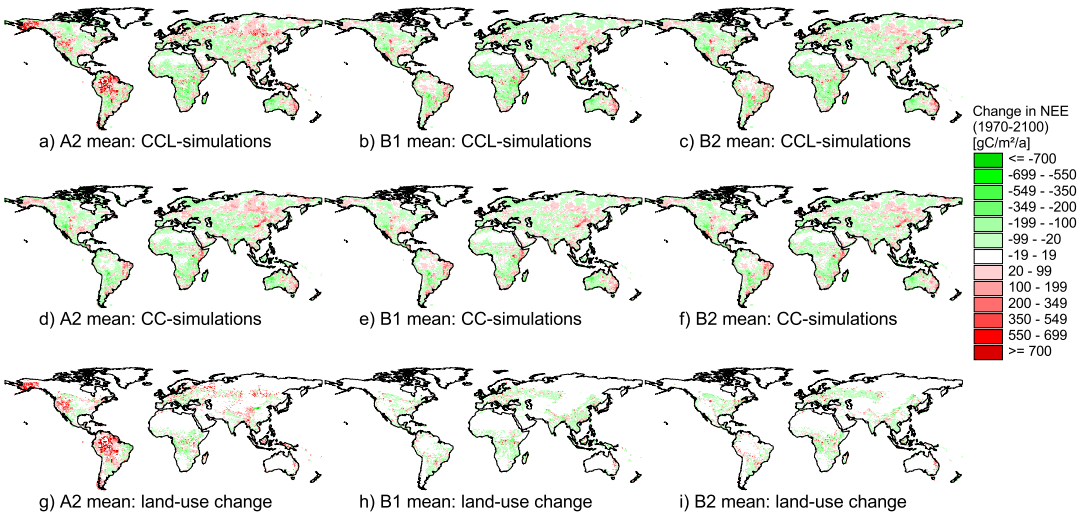

Figure 6. Mean changes in NEE averaged over the 4 different GCM scenarios from 1971-2000 (averaged) to 2071-2100 (averaged) for each SRES scenario. Negative values (green) indicate increased carbon sequestration or reduced carbon emissions, positive (red) vice versa.

Figure 7. Standard deviation of changes in NEE for the 3 SRES scenarios A2, B1 and B2 with 4 different climate patterns each for the CCL-simulations to demonstrate regional and local variance between the 4 different data sets for each SRES scenario.

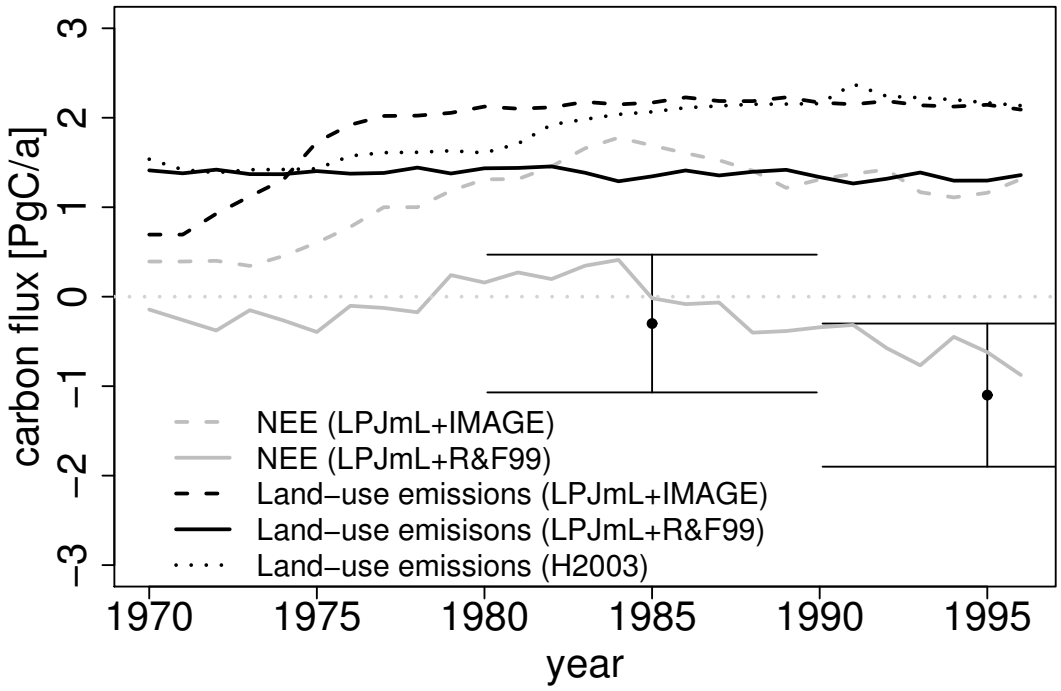

Figure 8. NEE and land-use emissions from 1970 to 1996 (10-year averages). LPJmL was used here with 2 different land-use data sets: the IMAGE 2.2 data set as used in this study (LPJmL+IMAGE) and the Ramankutty and Foley [1999] data set as used by Bondeau et al. [2007] (LPJmL+R&F99). Land-use emissions are compared with figures as reported by Houghton [2003] (H2003). The two points with error bars represent the uncertainty range of NEE estimates as reported by Schimel et al. [2001], Bopp et al. [2002], and Plattner et al. [2002] for the 1980s and 1990s respectively.